DSTBC based DF Cooperative Networks in the Presence of Timing and Frequency Offsets

Ali A. Nasir, Hani Mehrpouyan, Salman Durrani, Steven D. Blostein, Rodney A. Kennedy, and Björn Ottersten

Emails: ali.nasir@anu.edu.au, hani.mehr@ieee.org, salman.durrani@anu.edu.au, steven.blostein@queensu.ca, rodney.kennedy@anu.edu.au, and bjorn.ottersten@uni.lu

Abstract—In decode-and-forward (DF) relaying networks, the received signal at the destination may be affected by multiple impairments such as multiple channel gains, multiple timing offsets (MTOs), and multiple carrier frequency offsets (MCFOs). This paper proposes novel optimal and sub-optimal minimum mean-square error (MMSE) receiver designs at the destination node to detect the signal in the presence of these impairments. Distributed space-time block codes (DSTBCs) are used at the relays to achieve spatial diversity. The proposed sub-optimal receiver uses the estimated values of multiple channel gains, MTOs, and MCFOs, while the optimal receiver assumes perfect knowledge of these impairments at the destination and serves as a benchmark performance measure. To achieve robustness to estimation errors, the estimates statistical properties are exploited at the destination. Simulation results show that the proposed optimal and sub-optimal MMSE compensation receivers achieve full diversity gain in the presence of channel and synchronization impairments in DSTBC based DF cooperative networks.

I. INTRODUCTION

In distributed decode-and-forward (DF) multi-relay networks, the received signal at the destination is the superposition of the relays' transmitted signals that are attenuated differently, are no longer aligned with each other in time, and are experiencing phase rotations at different rates due to different channels, multiple timing offsets (MTOs), and multiple carrier frequency offsets (MCFOs) [1], [2]. Thus, joint estimation and compensation of these impairments is necessary to enable the detection of the received signal at the destination [2].

Different cooperation strategies have been employed at the relays. Relays can transmit sequentially in different time slots following the *repetition cooperative strategy* [3]. However, that leads to inefficient bandwidth utilization. Bandwidth efficiency can be improved by allowing the relays to transmit simultaneously. However, depending on how the relays' signals superimpose at the destination, achieving full diversity is not guaranteed [2], [4]. Recently, it has been shown that full diversity gains can be achieved by employing *distributed space-time block code (DSTBC) cooperative strategy*, which allows the relays to transmit in the same time slot using the DSTBC structure [5]–[7].

The joint estimation of multiple channel gains, MTOs, and MCFOs, in DF cooperative networks is well-studied in [2], [8]. However little research has been conducted on the development of compensation algorithms, which can detect the received signal by jointly compensating and removing the effect of multiple channel gains, MTOs, and MCFOs. Recent literature has addressed either MTO compensation [7] or MCFO compensation [9]–[11]. However, compensating one set of parameters does not result in successful signal detection in the presence of both MTOs and MCFOs. Even though joint synchronization schemes for compensating multiple channel gains, MTOs, and MCFOs for DF relaying DSTBC-orthogonal frequency division multiplexing (OFDM) based cooperative systems are available in the literature [12]–[14], these algorithms exploit the cyclic prefix and the frequency domain structure of the signal, which is specific to OFDM systems and depending on the number of sub-carriers used, the carrier frequency offset acquisition range of the algorithms is very limited. Finally, [2] addresses the problem of detection of the received signal from multiple relays in the presence of MTOs and MCFOs in DF cooperative systems. The decoding of the received signal is achieved through maximum likelihood (ML) approach. However, the complexity of ML decoding increases exponentially with constellation size, which limits the practical application of the detector in [2].

In this paper, our goal is to design a relay transmitter and an efficient receiver at the destination, which can compensate for the effect of multiple impairments and enable the detection of the received signal, while achieving full spatial diversity gain using DSTBCs. The main contributions of this paper can be summarized as follows:

- The transceiver structures at the relays and destination nodes for transmission of DSTBC in DF cooperative networks in the presence of MTOs and MCFOs is proposed.
- An MMSE receiver for compensating the effect of multiple channels gains, MTOs, and MCFOs and for detecting the signal from the relays at the destination is derived.
- Extensive simulations are carried out to investigate the performance of the proposed receiver design in DSTBC-DF cooperative networks for different numbers of relays. It is shown that the proposed DSTBC-DF relaying system achieves full spatial diversity gain for 2 and 4 relay networks and outperforms existing cooperative strategies in the presence of unknown channels, MTOs, and MCFOs.

Notation: Superscripts $(\cdot)^T$, $(\cdot)^H$, and $(\cdot)'$ denote the transpose, the conjugate transpose and the first derivative operators, respectively. $\odot$ and $\otimes$ stand for the Hadamard and Kronecker products, respectively. $\mathbb{E}_x\{\cdot\}$ denotes the expectation operator with respect to the variable x. Symbols with superscripts $(\cdot)^{[\text{TP}]}$ and $(\cdot)^{[\text{DTP}]}$ denote the signals in training and data transmission periods, respectively. The operator, $\hat{x}$ represents the estimated value of x. $\mathcal{N}(\mu, \sigma^2)$ and $\mathcal{CN}(\mu, \sigma^2)$ denote the real and complex Gaussian distributions with mean μ and variance σ^2, respectively.

Boldface small letters, $\mathbf{x}$ and boldface capital letters, $\mathbf{X}$ are used for vectors matrices, respectively. $\mathbf{I}_X$ and $\mathbf{0}_{X \times X}$ denote $X \times X$ identity and all zero matrices. $\|\mathbf{x}\|$ represents the ℓ_2 norm of a vector $\mathbf{x}$ and $\text{Tr}\{\mathbf{X}\}$ denotes the trace of $\mathbf{X}$. $\text{diag}(\mathbf{x})$ is used to denote a diagonal matrix, where its diagonal elements are given by the vector $\mathbf{x}$. $\mathcal{O}_p(\cdot)$ denotes the big omicron function for stochastic parameters [15]. Finally, $\boldsymbol{\Sigma}_{\mathbf{x}}$ and $\boldsymbol{\Phi}_{\mathbf{x}} \triangleq \mathbb{E}\{\mathbf{x}\mathbf{x}^H\}$ denote the covariance and correlation matrices of $\mathbf{x}$, respectively.

The remainder of the paper is organized as follows: Section II details the system model for the proposed DSTBC based DF relaying approach. Section III derives the MMSE receiver structure algorithms. Section IV presents numerical and simulation results. Finally, Section V summarizes the paper's key findings.

II. PROPOSED SYSTEM MODEL

A DF cooperative system comprising of one source node, $\mathbb{S}$, K relays, $\mathbb{R}_1, \ldots, \mathbb{R}_K$, and a single destination node, $\mathbb{D}$ is considered. All nodes are equipped with a single antenna. τ_k and ν_k are used to denote timing and frequency offsets, respectively, where superscripts $(\cdot)^{[\text{sr}]}$ and $(\cdot)^{[\text{rd}]}$ denote offsets from source to the kth relay and kth relay to destination, respectively. The channel gains from source to the kth relay and from kth relay to destination are denoted by ρ_k and η_k, respectively. Quasi-static and frequency flat fading channels are considered, i.e., the channel gains do not change over the length of a frame but change from frame to frame according to a complex Gaussian distribution, $\mathcal{CN}(0, \sigma^2)$. The use of such channels is motivated by the prior research in this field [7], [8], [16]. Throughout this paper, the index $k = 1, \ldots, K$ is used for K relays.
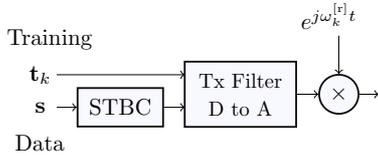

Fig. 1: Proposed DSTBC based DF transmitter at the kth relay.

The block diagram of the proposed DSTBC based DF transmitter at the kth relay is shown in Fig. 1. The block diagram of the DF receiver at the kth relay is described in [2] and, thus, is not repeated here. The estimation parameters ρ_k, $\tau_k^{[\text{sr}]}$, and $\nu_k^{[\text{sr}]}$, at the kth relay, can be jointly estimated and compensated using conventional schemes for single-input-single-output (SISO) point-to-point systems [17]. Thus, source to relay transmission will not be discussed in this paper. The transmission from relays to destination consists of two periods:

1) *Training period:* As shown in Fig. 1, during training period, each kth relay transmits the training signal $\mathbf{t}_k$ to the destination. The block diagram of the proposed DF receiver at the destination is shown in Fig. 2. Multiple channel gains $\eta_1, \ldots, \eta_K$, MTOs $\tau_1^{[\text{rd}]}, \ldots, \tau_K^{[\text{rd}]}$, and MC-FOs $\nu_1^{[\text{rd}]}, \ldots, \nu_K^{[\text{rd}]}$, are jointly estimated at the destination via the algorithm in [2].

2) *Data transmission period:* As shown in Fig. 1, each relay applies DSTBC to an M-phase shift keying (MPSK) modulated data signal, $\mathbf{s}$, where M is the constellation size. After applying DSTBC, each relay applies pulse shaping operation and up converts the analog signal by the oscillator frequency, $\omega_k^{[\text{r}]}$. At the destination, $y(t)$ is down converted
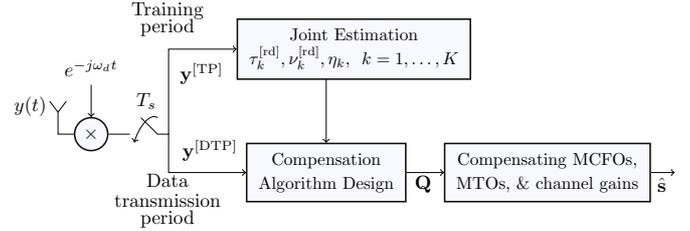

Fig. 2: Proposed DSTBC based receiver at the destination node.

by the oscillator frequency ω_d and then oversampled by the factor N (see Fig. 2).

During the data transmission period, the sampled received signal, $\mathbf{y}^{[\text{DTP}]}$, at the destination node is given by

$$\mathbf{y}^{[\text{DTP}]} = \boldsymbol{\Xi} \mathbf{A} \boldsymbol{\Omega} \mathbf{s} + \mathbf{w}, \tag{1}$$

where

- $\mathbf{y}^{[\text{DTP}]} \triangleq [y^{[\text{DTP}]}(0), \ldots, y^{[\text{DTP}]}(LN-1)]^T$, L denotes the number of data symbols, N is the oversampling factor,
- $\boldsymbol{\Xi} \triangleq [\boldsymbol{\Xi}_1, \ldots, \boldsymbol{\Xi}_K]$ is an $LN \times LK$ matrix, $\boldsymbol{\Xi}_k \triangleq \boldsymbol{\Lambda}_k \mathbf{G}_k$ is the $LN \times L$ matrix of the kth relay's frequency offset, $\nu_k^{[\text{rd}]}$, and timing offset, $\tau_k^{[\text{rd}]}$,
- $\boldsymbol{\Lambda}_k \triangleq \text{diag}\left([e^{j2\pi\nu_k^{[\text{rd}]}(0)/N}, \ldots, e^{j2\pi\nu_k^{[\text{rd}]}(LN-1)/N}]\right)$ is an $LN \times LN$ matrix, $\nu_k^{[\text{rd}]}$ denotes the normalized *unknown* frequency offset from the kth relay to the destination,
- $\mathbf{G}_k$ is the $LN \times L$ matrix of the samples of the pulse shaping filter such that $[\mathbf{G}_k]_{i,n} \triangleq g_{\text{rrc}}(iT_s - nT - \tau_k^{[\text{rd}]}T)$, $\tau_k^{[\text{rd}]}$ denotes the normalized fractional *unknown* timing offset between the kth relay and destination, $g_{\text{rrc}}(t)$ stands for the root raised-cosine pulse shaping function, T is the symbol duration, $T_s \triangleq T/N$ is the sampling period,
- $\mathbf{A} \triangleq \text{diag}(\eta_1, \ldots, \eta_K) \otimes \mathbf{I}_L$ is the $LK \times LK$ matrix of the *unknown* channel gains from relays to destination,
- $\boldsymbol{\Omega} \triangleq [\boldsymbol{\Omega}_1^H, \ldots, \boldsymbol{\Omega}_K^H]^H$ is an $LK \times L$ matrix, $\boldsymbol{\Omega}_k$ is the predefined $L \times L$ STBC matrix at the kth relay,
- $\mathbf{s} \triangleq [s(1), \ldots, s(L)]^T$ is an $L \times 1$ source data vector, which needs to be decoded at the destination,
- $\mathbf{w} \triangleq [w(0), \ldots, w(LN-1)]^T$ and $w(i) \,\forall\, i$, denotes the zero-mean complex additive white Gaussian noise (AWGN) at the ith sample of the received signal, i.e., $w(i) \sim \mathcal{CN}(0, \sigma_w^2)$.

As shown in (1), the received signal, $\mathbf{y}^{[\text{DTP}]}$, is the superposition of the relays' transmitted signals that are attenuated differently, are no longer aligned with each other in time, and are experiencing phase rotations at different rates due to different channels, $\boldsymbol{\eta} \triangleq [\eta_1, \ldots, \eta_K]^T$, MTOs, $\boldsymbol{\tau}^{[\text{rd}]} \triangleq \left[\tau_1^{[\text{rd}]}, \ldots, \tau_K^{[\text{rd}]}\right]^T$, and MCFOs, $\boldsymbol{\nu}^{[\text{rd}]} \triangleq \left[\nu_1^{[\text{rd}]}, \ldots, \nu_K^{[\text{rd}]}\right]^T$. Our goal is to design an efficient receiver at the destination that compensate the effect of these impairments and enable the detection of data signal $\mathbf{s}$, while achieving full spatial diversity gain using DSTBCs.

III. PROPOSED COMPENSATION ALGORITHM

In this section, sub-optimal and optimal MMSE compensation algorithms for signal detection in DSTBC based DF cooperative networks are derived.

A. Sub-optimal MMSE Compensation

The multiple channel gains, $\hat{\boldsymbol{\eta}}$, MTOs, $\hat{\boldsymbol{\tau}}^{[\text{rd}]}$, and MCFOs, $\hat{\boldsymbol{\nu}}^{[\text{rd}]}$, for the proposed sub-optimal compensation algorithm can

be estimated during the training period using the maximum likelihood (ML) algorithm derived in [2]. These impairments, however, suffer from random estimation errors, i.e., $\boldsymbol{\delta}_{\boldsymbol{\eta}} = \boldsymbol{\eta} - \hat{\boldsymbol{\eta}}$, $\boldsymbol{\delta}_{\boldsymbol{\tau}^{[\mathrm{rd}]}} = \boldsymbol{\tau}^{[\mathrm{rd}]} - \hat{\boldsymbol{\tau}}^{[\mathrm{rd}]}$, and $\boldsymbol{\delta}_{\boldsymbol{\nu}^{[\mathrm{rd}]}} = \boldsymbol{\nu}^{[\mathrm{rd}]} - \hat{\boldsymbol{\nu}}^{[\mathrm{rd}]}$. In order to make the compensation algorithm robust to these estimation errors, $(\boldsymbol{\delta}_{\boldsymbol{\eta}}, \boldsymbol{\delta}_{\boldsymbol{\tau}^{[\mathrm{rd}]}}, \boldsymbol{\delta}_{\boldsymbol{\nu}^{[\mathrm{rd}]}})$, their statistical properties can be exploited at the receiver. Since, an ML estimator asymptotically efficient [18], the estimation errors can be modeled as a multi-variate Gaussian distribution, i.e., $\boldsymbol{\delta}_{\boldsymbol{\eta}} \sim \mathcal{CN}\left(\mathbf{0}_{K \times 1}, \mathbf{CRLB}(\boldsymbol{\eta})\right)$, $\boldsymbol{\delta}_{\boldsymbol{\tau}^{[\mathrm{rd}]}} \sim \mathcal{N}\left(\mathbf{0}_{K \times 1}, \mathbf{CRLB}(\boldsymbol{\tau}^{[\mathrm{rd}]})\right)$, $\boldsymbol{\delta}_{\boldsymbol{\nu}^{[\mathrm{rd}]}} \sim \mathcal{N}\left(\mathbf{0}_{K \times 1}, \mathbf{CRLB}(\boldsymbol{\nu}^{[\mathrm{rd}]})\right)$, where $\mathbf{CRLB}(\boldsymbol{\eta})$, $\mathbf{CRLB}(\boldsymbol{\tau}^{[\mathrm{rd}]})$, and $\mathbf{CRLB}(\boldsymbol{\nu}^{[\mathrm{rd}]})$ are $K \times K$ Cramér-Rao lower bound (CRLB) matrices for the estimation of channels gains, MTOs, and MCFOs, respectively, and are derived in [2, Eq. (19)].

Theorem: The sub-optimal MMSE compensation matrix, $\mathbf{Q}^{[\mathrm{MMSE}]}$, is determined by minimizing the cost function

$$\chi^{\mathrm{MMSE}} = \mathbb{E}_{\boldsymbol{\delta}_{\boldsymbol{\eta}}, \boldsymbol{\delta}_{\boldsymbol{\nu}^{[\mathrm{rd}]}}, \boldsymbol{\delta}_{\boldsymbol{\tau}^{[\mathrm{rd}]}}, \mathbf{w}, \mathbf{s}} \left\{ \|\mathbf{Q}\mathbf{y}^{[\mathrm{DTP}]} - \mathbf{s}\|^2 \right\}, \qquad (2)$$

and is given by

$$\mathbf{Q}^{[\mathrm{MMSE}]} = \boldsymbol{\Phi}_{\mathbf{s}}^H \boldsymbol{\Omega}^H \hat{\mathbf{A}}^H \hat{\boldsymbol{\Xi}}^H \left(\hat{\boldsymbol{\Xi}} \mathbf{R} \hat{\boldsymbol{\Xi}}^H + \boldsymbol{\Sigma}_{\mathbf{w}} \right)^{-1}, \qquad (3)$$

where $\boldsymbol{\Phi}_{\mathbf{s}} \triangleq \mathbb{E}_{\mathbf{s}}\left\{ \mathbf{s}\mathbf{s}^H \right\}$ and $\boldsymbol{\Sigma}_{\mathbf{w}} \triangleq \mathbb{E}_{\mathbf{w}}\left\{ \mathbf{w}\mathbf{w}^H \right\}$.

Proof: See Appendix A.

By applying the compensation matrix, $\mathbf{Q}^{[\mathrm{MMSE}]}$, to the received signal, $\mathbf{y}^{\mathrm{DTP}}$, the effect of multiple channels, MTOs, and MCFOs is removed from the decoded signal, $\hat{\mathbf{s}} = \mathbf{Q}^{[\mathrm{MMSE}]}\mathbf{y}^{\mathrm{DTP}}$.

B. Optimal MMSE Compensation

In order to benchmark the performance of the proposed sub-optimal MMSE compensation algorithm, one can formulate an optimal MMSE receiver that is derived based on the assumption of perfect knowledge of multiple channel gains, MTOs, and MCFOs at the destination, i.e., $\boldsymbol{\delta}_{\boldsymbol{\eta}} = \boldsymbol{\delta}_{\boldsymbol{\tau}^{[\mathrm{rd}]}} = \boldsymbol{\delta}_{\boldsymbol{\nu}^{[\mathrm{rd}]}} = \mathbf{0}_{K \times 1}$. Based on this assumption, the optimal compensation matrix, $\mathbf{Q}^{[\mathrm{OPT}]}$, can be obtained by minimizing the following cost function, χ^{OPT}, below

$$\chi^{\mathrm{OPT}} = \mathbb{E}_{\mathbf{w}, \mathbf{s}} \left\{ \|\mathbf{Q}^{[\mathrm{OPT}]}\mathbf{y}^{[\mathrm{DTP}]} - \mathbf{s}\|^2 \right\}, \qquad (4)$$

where the expectation in (4) is taken with respect to the statistics of $\mathbf{w}$ and $\mathbf{s}$. Substituting (1) into (4), the cost function, χ^{OPT}, is given by

$$\begin{aligned}
\chi^{\mathrm{OPT}} = \mathrm{Tr}\Big\{ &\mathbf{Q}^{[\mathrm{OPT}]}\boldsymbol{\Xi}\mathbf{A}\boldsymbol{\Omega}\boldsymbol{\Phi}_{\mathbf{s}}\boldsymbol{\Omega}^H\mathbf{A}^H\boldsymbol{\Xi}^H\left(\mathbf{Q}^{[\mathrm{OPT}]}\right)^H + \boldsymbol{\Phi}_{\mathbf{s}} \\
&+ \mathbf{Q}^{[\mathrm{OPT}]}\boldsymbol{\Sigma}_{\mathbf{w}}\left(\mathbf{Q}^{[\mathrm{OPT}]}\right)^H - \mathbf{Q}^{[\mathrm{OPT}]}\boldsymbol{\Xi}\mathbf{A}\boldsymbol{\Omega}\boldsymbol{\Phi}_{\mathbf{s}} \\
&- \boldsymbol{\Phi}_{\mathbf{s}}^H\boldsymbol{\Omega}^H\mathbf{A}^H\boldsymbol{\Xi}^H\left(\mathbf{Q}^{[\mathrm{OPT}]}\right)^H \Big\}. \qquad (5)
\end{aligned}$$

By taking the derivative of χ^{OPT} in (5) with respect to $\left(\mathbf{Q}^{[\mathrm{OPT}]}\right)^H$ and setting the result to zero, the optimal compensation matrix, $\mathbf{Q}^{[\mathrm{OPT}]}$, is derived as

$$\mathbf{Q}^{[\mathrm{OPT}]} = \boldsymbol{\Phi}_{\mathbf{s}}^H\boldsymbol{\Omega}^H\mathbf{A}^H\boldsymbol{\Xi}^H\left(\boldsymbol{\Xi}\mathbf{A}\boldsymbol{\Omega}\boldsymbol{\Phi}_{\mathbf{s}}\boldsymbol{\Omega}^H\mathbf{A}^H\boldsymbol{\Xi}^H + \boldsymbol{\Sigma}_{\mathbf{w}}\right)^{-1}. \quad (6)$$

The decoded signal for the optimal benchmark receiver is given by $\hat{\mathbf{s}} = \mathbf{Q}^{[\mathrm{OPT}]}\mathbf{y}^{[\mathrm{DTP}]}$.

IV. SIMULATION RESULTS

In this section, we investigate the receiver performance at the destination, where multiple channel gains, MTOs, and MCFOs are jointly estimated and compensated in order to decode the received signal. In our simulation setup, we consider $K = 2$ and 4 relays in DF cooperative systems. Quadrature phase-shift keying modulation (QPSK) is employed for data transmission. Length of the training signal, $\mathbf{t}_k^{[\mathrm{rd}]}, \forall k$, is set to $L = 80$ symbols during training period and length of the source data vector $\mathbf{s}$, is set to $L = 400$ symbols during data transmission period, resulting in a synchronization overhead of 16%. Oversampling factor is set to $N = 2$ and a root-raised cosine filter with a roll-off factor of 0.22 is employed. At each relay, the DSTBC is generated randomly based on an isotropic distribution on the space of $L \times L$ unitary matrices, which is a benchmark method for generating DSTBC in cooperative networks [5], [6]. The propagation loss is modeled as $\alpha = (d/d_0)^{-m}$, where d is the distance between transmitter and receiver, d_0 is the reference distance, and m is the path loss exponent [17]. We set $d_0 = 1$ km, and $m = 2.7$, which corresponds to urban area cellular networks [17]. The timing and frequency offsets at the destination, $\boldsymbol{\tau}^{[\mathrm{rd}]}$ and $\boldsymbol{\nu}^{[\mathrm{rd}]}$, are uniformly drawn from the full acquisition range, $(-0.5, 0.5)$.

Fig. 3 and Fig. 4 demonstrate the bit error rate (BER) performance of the proposed sub-optimal and optimal MMSE compensation receivers for 2 and 4-relays networks, respectively. For the proposed sub-optimal MMSE receiver the ML estimator is used to obtain the estimates of multiple channel parameters, MTOs, and MCFOs. The BER performance of the proposed receivers with and without the use of DSTBCs is presented. Fig. 3 and Fig. 4 show improvement in BER results in the presence of DSTBCs, e.g., considering sub-optimal MMSE compensation at BER $= 4 \times 10^{-5}$, the receiver employing DSTBC outperforms the BER performance of the receiver without DSTBC by 6 and 8 dB for 2 and 4-relays networks, respectively. Fig. 3 and Fig. 4 also show that the BER of a DSTBC based cooperative system based on the estimated impairments is close to that of the ideal scenario with perfect knowledge of impairments and optimal compensation, i.e., a performance gap of 3 and 6 dB for 2 and 4-relays cooperative systems, respectively.

Fig. 5 shows the BER performance of the proposed sub-optimal MMSE receiver for $K = 2$ and 4 relays. Fig. 5 also plots the BER results for a cooperative system that first employs the re-synchronization filter in [7] to compensate MTOs and then attempts to remove MCFOs by employing the algorithm in [10]. Fig. 5 shows that such a compensation approach, which is denoted by "[7] & [10], K=2", fails to decode the received signal at the destination since the re-synchronization filter in [7] fails to compensate MTOs in the presence of MCFOs. Subsequently, the algorithm in [10] fails to nullify MCFOs, since the input signal is corrupted by MTOs. In addition, Fig. 5 also illustrates the BER performance of a cooperative system applying the ML decoding based receiver in [2], for 2 and 4 relays. It can be observed from Fig. 5 that the proposed receiver outperforms that of [2] by 3 and 10 dB at a BER $= 1 \times 10^{-5}$ for 2 and 4 relay cooperative networks, respectively. Moreover, there is no spatial diversity gain exhibited by the BER performance of [2]. On the other hand, Fig. 5 shows that the proposed MMSE receiver for $K = 2$ and 4 relays achieves full spatial diversity.
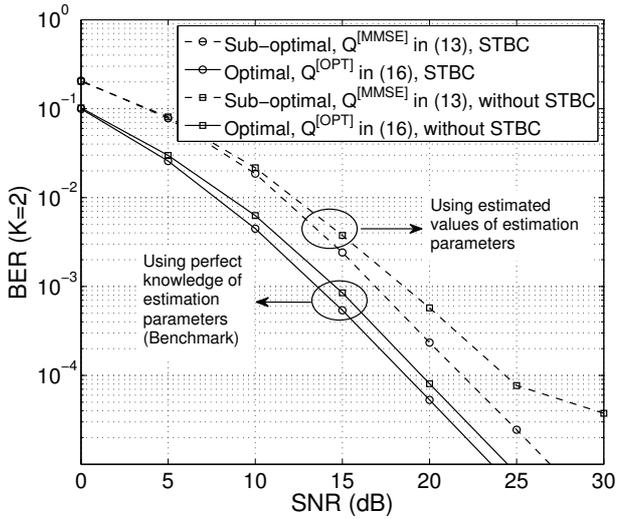
Fig. 3: BER of the proposed MMSE and optimal benchmark receivers for 2-relay DF cooperative network with and without DSTBCs.

Fig. 4: BER of the proposed MMSE and optimal benchmark receivers for 4-relay DF cooperative network with and without DSTBCs.

TABLE I

CPU PROCESSING TIME FOR THE PROPOSED SUB-OPTIMAL MMSE COMPENSATION ALGORITHM AND ML DECODING ALGORITHM IN [2] AT SNR = 30 dB USING INTEL CORE I7-2670QM, 2.20 GHz PROCESSOR

No. of Relays (K)	Proposed Algorithm (seconds)	[2] (seconds)
2	3.7	68.2
4	11.2	126.06

The proposed receiver not only demonstrates better BER performance compared to existing compensation methods, but is also computationally more efficient compared to the ML algorithm in [2]. The computational complexities of the proposed sub-optimal MMSE compensation method and ML decoding algorithm in [2] are evaluated using CPU execution time [19]. As shown in Table I, the execution time is observed at SNR = 30 dB, when an Intel Core i7 − 2670QM, 2.20 GHz processor with 8 GB of RAM is used. It has been observed that compared to the decoding algorithm in [2], the proposed MMSE compensation method is capable of compensating the effect of multiple impairments and decoding the received signal approximately 18 and 11 times more quickly for 2 and 4 relay cooperative network respectively. *It is important to mention here that in [2], our focus was on the joint estimation of multiple channel gains, MTOs, and MCFOs at the destination. The design of efficient algorithms for joint compensation of multiple impairments was left as a subject of future research and has been discussed in this paper.*

V. CONCLUSIONS

This paper has proposed novel optimal and sub-optimal MMSE receiver designs at the destination node in DF cooperative networks in the presence of multiple channel gains, MTOs, and MCFOs. In order to make the sub-optimal compensation algorithm robust to the estimation errors, the statistical properties of estimation errors are exploited at the destination. Simulation results show that the proposed optimal and sub-optimal MMSE compensation receivers achieve full diversity gain in the presence of channel and synchronization impairments in DSTBC based DF
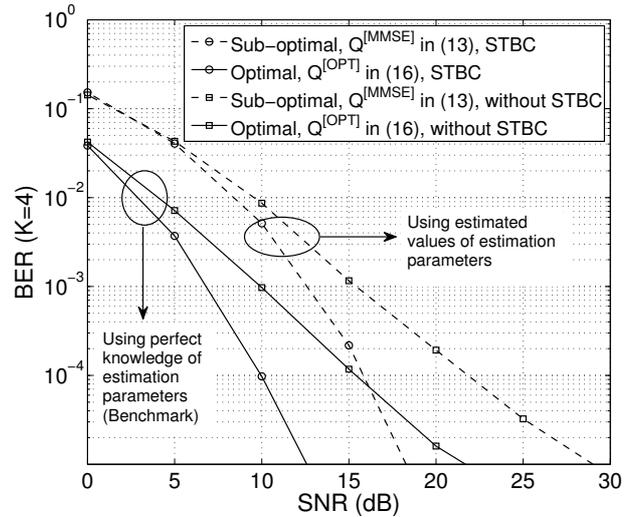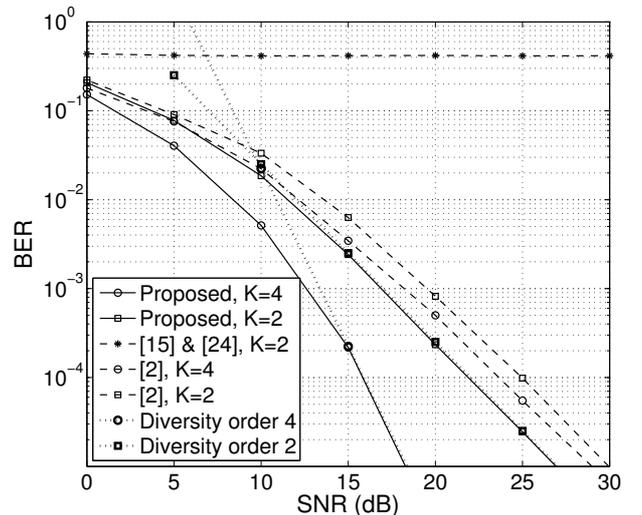

Fig. 5: BER performance comparison of the proposed sub-optimal compensation algorithm, $\mathbf{Q}^{[MMSE]}$ in (3), with the previous methods for $K = 2$ and 4 relays cooperative system

cooperative networks. The performance of the proposed receiver has also been compared with the existing receivers. The simulation results demonstrate that the proposed sub-optimal MMSE receiver not only promises performance gain in terms of system BER over existing receiver but also offers 18 and 11 times more computational efficiency, while simulating 2 and 4 relays DF cooperative system, respectively, with QPSK modulation and 10% synchronization overhead.

APPENDIX A
PROOF OF THEOREM 1

In (2), the expectation is taken with respect to the statistics of the estimation errors, $\delta_{\boldsymbol{\eta}}$, $\delta_{\boldsymbol{\nu}^{[rd]}}$, $\delta_{\boldsymbol{\tau}^{[rd]}}$, and $\mathbf{w}$ and $\mathbf{s}$. Furthermore, it is assumed that $\mathrm{Tr}\left\{\mathbb{E}_{\mathbf{s}}\left\{\mathbf{s}\mathbf{s}^{H}\right\}\right\} \leq L$, to meet the power constraint

at the destination. Substituting (1) in (2), we have

$$\chi^{\text{MMSE}} = \mathbb{E}_{\boldsymbol{\delta}_{\boldsymbol{\eta}}, \boldsymbol{\delta}_{\boldsymbol{\nu}^{[\text{rd}]}}, \boldsymbol{\delta}_{\boldsymbol{\tau}^{[\text{rd}]}}, \mathbf{w}, \mathbf{s}} \left\{ \| \mathbf{Q} \left(\boldsymbol{\Xi} \mathbf{A} \boldsymbol{\Omega} \mathbf{s} + \mathbf{w} \right) - \mathbf{s} \|^2 \right\}. \quad \text{(A.1)}$$

Since, $\mathbf{s}$ and $\mathbf{w}$ are uncorrelated, (A.1) can be expanded as

$$\chi^{\text{MMSE}} = \text{Tr}\Big\{ \mathbf{Q} \mathbb{E}_{\boldsymbol{\delta}_{\boldsymbol{\tau}^{[\text{rd}]}}, \boldsymbol{\delta}_{\boldsymbol{\nu}^{[\text{rd}]}}} \left\{ \boldsymbol{\Xi} \mathbb{E}_{\boldsymbol{\delta}_{\boldsymbol{\eta}}} \left\{ \mathbf{A} \boldsymbol{\Omega} \boldsymbol{\Phi}_{\mathbf{s}} \boldsymbol{\Omega}^H \mathbf{A}^H \right\} \boldsymbol{\Xi}^H \right\} \mathbf{Q}^H$$
$$- \mathbf{Q} \mathbb{E}_{\boldsymbol{\delta}_{\boldsymbol{\tau}^{[\text{rd}]}}, \boldsymbol{\delta}_{\boldsymbol{\nu}^{[\text{rd}]}}} \left\{ \boldsymbol{\Xi} \mathbb{E}_{\boldsymbol{\delta}_{\boldsymbol{\eta}}} \left\{ \mathbf{A} \boldsymbol{\Omega} \boldsymbol{\Phi}_{\mathbf{s}} \right\} \right\}$$
$$- \mathbb{E}_{\boldsymbol{\delta}_{\boldsymbol{\tau}^{[\text{rd}]}}, \boldsymbol{\delta}_{\boldsymbol{\nu}^{[\text{rd}]}}} \left\{ \mathbb{E}_{\boldsymbol{\delta}_{\boldsymbol{\eta}}} \left\{ \boldsymbol{\Phi}_{\mathbf{s}}^H \boldsymbol{\Omega}^H \mathbf{A}^H \right\} \boldsymbol{\Xi}^H \right\} \mathbf{Q}^H$$
$$+ \boldsymbol{\Phi}_{\mathbf{s}} + \mathbf{Q} \boldsymbol{\Sigma}_{\mathbf{w}} \mathbf{Q}^H \Big\}, \quad \text{(A.2)}$$

where $\boldsymbol{\Phi}_{\mathbf{s}} \triangleq \mathbb{E}_{\mathbf{s}} \left\{ \mathbf{s} \mathbf{s}^H \right\}$ because the transmitted data symbols are assumed to be uncorrelated and $\boldsymbol{\Sigma}_{\mathbf{w}} \triangleq \mathbb{E}_{\mathbf{w}} \left\{ \mathbf{w} \mathbf{w}^H \right\}$. Since $\boldsymbol{\delta}_{\boldsymbol{\eta}} = \boldsymbol{\eta} - \hat{\boldsymbol{\eta}}$, the channel matrix $\mathbf{A}$, given below (1), can be written as $\mathbf{A} = \hat{\mathbf{A}} + \boldsymbol{\Delta}_{\mathbf{A}}$, where $\hat{\mathbf{A}} \triangleq \text{diag}\left(\hat{\boldsymbol{\eta}} \right) \otimes \mathbf{I}_L$ and $\boldsymbol{\Delta}_{\mathbf{A}} \triangleq \text{diag}\left(\boldsymbol{\delta}_{\boldsymbol{\eta}} \right) \otimes \mathbf{I}_L$ are $LK \times LK$ matrices. Using the distribution of $\boldsymbol{\delta}_{\boldsymbol{\eta}}$, $\mathbb{E}_{\boldsymbol{\delta}_{\boldsymbol{\eta}}} \left\{ \mathbf{A} \boldsymbol{\Omega} \boldsymbol{\Phi}_{\mathbf{s}} \boldsymbol{\Omega}^H \mathbf{A}^H \right\}$ and $\mathbb{E}_{\boldsymbol{\delta}_{\boldsymbol{\eta}}} \left\{ \mathbf{A} \boldsymbol{\Omega} \boldsymbol{\Phi}_{\mathbf{s}} \right\}$ are evaluated as

$$\mathbb{E}_{\boldsymbol{\delta}_{\boldsymbol{\eta}}} \left\{ \mathbf{A} \boldsymbol{\Omega} \boldsymbol{\Phi}_{\mathbf{s}} \boldsymbol{\Omega}^H \mathbf{A}^H \right\} = \hat{\mathbf{A}} \boldsymbol{\Omega} \boldsymbol{\Phi}_{\mathbf{s}} \boldsymbol{\Omega}^H \hat{\mathbf{A}}^H \quad \text{(A.3a)}$$
$$+ \left(\text{CRLB}\left(\hat{\boldsymbol{\eta}} \right) \otimes \mathbf{I}_L \right) \odot \left(\boldsymbol{\Omega} \boldsymbol{\Phi}_{\mathbf{s}} \boldsymbol{\Omega}^H \right),$$
$$\mathbb{E}_{\boldsymbol{\delta}_{\boldsymbol{\eta}}} \left\{ \mathbf{A} \boldsymbol{\Omega} \boldsymbol{\Phi}_{\mathbf{s}} \right\} = \hat{\mathbf{A}} \boldsymbol{\Omega} \boldsymbol{\Phi}_{\mathbf{s}}. \quad \text{(A.3b)}$$

where $\text{CRLB}\left(\hat{\boldsymbol{\eta}} \right)$ is a $K \times K$ matrix obtained by evaluating $\text{CRLB}\left(\boldsymbol{\eta} \right)$ in [2, Eq. (19)] by substituting $\hat{\boldsymbol{\eta}}$, $\hat{\boldsymbol{\tau}}^{[\text{rd}]}$, and $\hat{\boldsymbol{\nu}}^{[\text{rd}]}$ for $\boldsymbol{\eta}$, $\boldsymbol{\tau}^{[\text{rd}]}$, and $\boldsymbol{\nu}^{[\text{rd}]}$, respectively.

In order to evaluate $\mathbb{E}_{\boldsymbol{\delta}_{\boldsymbol{\tau}^{[\text{rd}]}}, \boldsymbol{\delta}_{\boldsymbol{\nu}^{[\text{rd}]}}} \left\{ \boldsymbol{\Xi} \mathbb{E}_{\boldsymbol{\delta}_{\boldsymbol{\eta}}} \left\{ \mathbf{A} \boldsymbol{\Omega} \boldsymbol{\Phi}_{\mathbf{s}} \boldsymbol{\Omega}^H \mathbf{A}^H \right\} \boldsymbol{\Xi}^H \right\}$, let us define an $LK \times LK$ matrix $\mathbf{Z} \triangleq \mathbb{E}_{\boldsymbol{\delta}_{\boldsymbol{\eta}}} \left\{ \mathbf{A} \boldsymbol{\Omega} \boldsymbol{\Phi}_{\mathbf{s}} \boldsymbol{\Omega}^H \mathbf{A}^H \right\}$ containing $L \times L$ square submatrices $\mathbf{Z}_{k,\bar{k}}$, for $k, \bar{k} = 1, \dots, K$. Thus, $\mathbb{E}_{\boldsymbol{\delta}_{\boldsymbol{\tau}^{[\text{rd}]}}, \boldsymbol{\delta}_{\boldsymbol{\nu}^{[\text{rd}]}}} \left\{ \boldsymbol{\Xi} \mathbf{Z} \boldsymbol{\Xi}^H \right\}$ can be expressed as

$$\mathbb{E}_{\boldsymbol{\delta}_{\boldsymbol{\tau}^{[\text{rd}]}}, \boldsymbol{\delta}_{\boldsymbol{\nu}^{[\text{rd}]}}} \left\{ \boldsymbol{\Xi} \mathbf{Z} \boldsymbol{\Xi}^H \right\} = \sum_{k,\bar{k}=1}^{K} \mathbb{E}_{\boldsymbol{\delta}_{\boldsymbol{\tau}^{[\text{rd}]}}, \boldsymbol{\delta}_{\boldsymbol{\nu}^{[\text{rd}]}}} \left\{ \boldsymbol{\Xi}_k \mathbf{Z}_{k,\bar{k}} \boldsymbol{\Xi}_{\bar{k}} \right\}. \quad \text{(A.4)}$$

Note that $\boldsymbol{\Xi}_k \triangleq \boldsymbol{\Lambda}_k \mathbf{G}_k$ is a non-linear function of $\tau_k^{[\text{rd}]}$ and $\nu_k^{[\text{rd}]}$. Thus, in order to evaluate (A.4), the Taylor series expansion of the non-linear terms $\boldsymbol{\Lambda}_k$ and $\mathbf{G}_k$ around $\nu_k^{[\text{rd}]}$ and $\tau_k^{[\text{rd}]}$, respectively, can be evaluated as

$$\boldsymbol{\Lambda}_k = \hat{\boldsymbol{\Lambda}}_k + \hat{\boldsymbol{\Lambda}}_k' \delta_{\nu_k^{[\text{rd}]}} + \mathcal{O}_p \left(\sigma_{\nu_k^{[\text{rd}]}}^2 \right), \quad \text{(A.5a)}$$
$$\mathbf{G}_k = \hat{\mathbf{G}}_k + \hat{\mathbf{G}}_k' \delta_{\tau_k^{[\text{rd}]}} + \mathcal{O}_p \left(\sigma_{\tau_k^{[\text{rd}]}}^2 \right), \quad \text{(A.5b)}$$

where $\hat{\boldsymbol{\Lambda}}_k \triangleq \boldsymbol{\Lambda}_k \big|_{\nu_k^{[\text{rd}]} = \hat{\nu}_k^{[\text{rd}]}}$, $\hat{\mathbf{G}}_k \triangleq \mathbf{G}_k \big|_{\tau_k^{[\text{rd}]} = \hat{\tau}_k^{[\text{rd}]}}$, $\hat{\boldsymbol{\Lambda}}_k' \triangleq \frac{\partial \boldsymbol{\Lambda}_k}{\partial \nu_k^{[\text{rd}]}} \big|_{\nu_k^{[\text{rd}]} = \hat{\nu}_k^{[\text{rd}]}} \mathcal{O}_p \left(\cdot \right)$, $\hat{\mathbf{G}}_k' \triangleq \frac{\partial \mathbf{G}_k}{\partial \tau_k^{[\text{rd}]}} \big|_{\tau_k^{[\text{rd}]} = \hat{\tau}_k^{[\text{rd}]}}$, and $\sigma_{\nu_k^{[\text{rd}]}}^2$ and $\sigma_{\tau_k^{[\text{rd}]}}^2$ are frequency and timing offset estimation error variances, respectively, given by the kth diagonal element of $\text{CRLB}(\boldsymbol{\nu}^{[\text{rd}]})$ and $\text{CRLB}(\boldsymbol{\tau}^{[\text{rd}]})$, respectively. Using (A.5), $\boldsymbol{\Xi}_k$ is evaluated as

$$\boldsymbol{\Xi}_k = \hat{\boldsymbol{\Lambda}}_k \hat{\mathbf{G}}_k + \delta_{\nu_k^{[\text{rd}]}} \hat{\boldsymbol{\Lambda}}_k' \hat{\mathbf{G}}_k + \delta_{\tau_k^{[\text{rd}]}} \hat{\boldsymbol{\Lambda}}_k \hat{\mathbf{G}}_k'$$
$$+ \delta_{\nu_k^{[\text{rd}]}} \delta_{\tau_k^{[\text{rd}]}} \hat{\boldsymbol{\Lambda}}_k' \hat{\mathbf{G}}_k' + \mathcal{O}_p \left(\sigma_{\tau_k^{[\text{rd}]}}^2 \right), \quad \text{(A.6)}$$

where, among $\sigma_{\tau_k^{[\text{rd}]}}^2$ and $\sigma_{\nu_k^{[\text{rd}]}}^2$, big omicron function for the dominant factor, $\sigma_{\tau_k^{[\text{rd}]}}^2$, is used in (A.6). Using (A.6) and by neglecting the higher order terms, $\mathbb{E}_{\boldsymbol{\delta}_{\boldsymbol{\tau}^{[\text{rd}]}}, \boldsymbol{\delta}_{\boldsymbol{\nu}^{[\text{rd}]}}} \left\{ \boldsymbol{\Xi}_k \mathbf{Z}_{k,\bar{k}} \boldsymbol{\Xi}_{\bar{k}} \right\}$ can be approximated as

$$\mathbb{E}_{\boldsymbol{\delta}_{\boldsymbol{\tau}^{[\text{rd}]}}, \boldsymbol{\delta}_{\boldsymbol{\nu}^{[\text{rd}]}}} \left\{ \boldsymbol{\Xi}_k \mathbf{Z}_{k,\bar{k}} \boldsymbol{\Xi}_{\bar{k}} \right\} = \hat{\boldsymbol{\Lambda}}_k \hat{\mathbf{G}}_k \mathbf{Z}_{k,\bar{k}} \hat{\mathbf{G}}_{\bar{k}}^H \hat{\boldsymbol{\Lambda}}_{\bar{k}}^H + \mathcal{O}_p \left(\sigma_{\tau_k^{[\text{rd}]}}^2 \right)$$
$$\approx \hat{\boldsymbol{\Lambda}}_k \hat{\mathbf{G}}_k \mathbf{Z}_{k,\bar{k}} \hat{\mathbf{G}}_{\bar{k}}^H \hat{\boldsymbol{\Lambda}}_{\bar{k}}^H, \quad \text{(A.7)}$$

where $\hat{\boldsymbol{\Xi}}_{\bar{k}} \triangleq \hat{\boldsymbol{\Lambda}}_k \hat{\mathbf{G}}_k$. Similarly, $\mathbb{E}_{\boldsymbol{\delta}_{\boldsymbol{\tau}^{[\text{rd}]}}, \boldsymbol{\delta}_{\boldsymbol{\nu}^{[\text{rd}]}}} \left\{ \boldsymbol{\Xi}_k \right\} \triangleq \hat{\boldsymbol{\Xi}}_k$. Using (A.4) and (A.6), $\mathbb{E}_{\boldsymbol{\delta}_{\boldsymbol{\tau}^{[\text{rd}]}}, \boldsymbol{\delta}_{\boldsymbol{\nu}^{[\text{rd}]}}} \left\{ \boldsymbol{\Xi} \mathbb{E}_{\boldsymbol{\delta}_{\boldsymbol{\eta}}} \left\{ \mathbf{A} \boldsymbol{\Omega} \boldsymbol{\Phi}_{\mathbf{s}} \boldsymbol{\Omega}^H \mathbf{A}^H \right\} \boldsymbol{\Xi}^H \right\}$ can be approximated as

$$\mathbb{E}_{\boldsymbol{\delta}_{\boldsymbol{\tau}^{[\text{rd}]}}, \boldsymbol{\delta}_{\boldsymbol{\nu}^{[\text{rd}]}}} \left\{ \boldsymbol{\Xi} \mathbb{E}_{\boldsymbol{\delta}_{\boldsymbol{\eta}}} \left\{ \mathbf{A} \boldsymbol{\Omega} \boldsymbol{\Phi}_{\mathbf{s}} \boldsymbol{\Omega}^H \mathbf{A}^H \right\} \boldsymbol{\Xi}^H \right\}$$
$$\approx \hat{\boldsymbol{\Xi}} \mathbb{E}_{\boldsymbol{\delta}_{\boldsymbol{\eta}}} \left\{ \mathbf{A} \boldsymbol{\Omega} \boldsymbol{\Phi}_{\mathbf{s}} \boldsymbol{\Omega}^H \mathbf{A}^H \right\} \hat{\boldsymbol{\Xi}}^H. \quad \text{(A.8)}$$

By combining the results derived in (A.5) and (A.8), the cost function in (A.2) can be approximated as

$$\chi^{\text{MMSE}} \approx \text{Tr}\Big\{ \mathbf{Q} \hat{\boldsymbol{\Xi}} \mathbf{R} \hat{\boldsymbol{\Xi}}^H \mathbf{Q}^H + \mathbf{Q} \boldsymbol{\Sigma}_{\mathbf{w}} \mathbf{Q}^H + \boldsymbol{\Phi}_{\mathbf{s}}$$
$$- \mathbf{Q} \hat{\boldsymbol{\Xi}} \hat{\mathbf{A}} \boldsymbol{\Omega} \boldsymbol{\Phi}_{\mathbf{s}} - \boldsymbol{\Phi}_{\mathbf{s}}^H \boldsymbol{\Omega}^H \hat{\mathbf{A}}^H \hat{\boldsymbol{\Xi}}^H \mathbf{Q}^H \Big\}, \quad \text{(A.9)}$$

where $\mathbf{R} = \hat{\mathbf{A}} \boldsymbol{\Omega} \boldsymbol{\Phi}_{\mathbf{s}} \boldsymbol{\Omega}^H \hat{\mathbf{A}}^H + \left(\text{CRLB}(\hat{\boldsymbol{\eta}}) \otimes \mathbf{I}_L \right) \odot \left(\boldsymbol{\Omega} \boldsymbol{\Phi}_{\mathbf{s}} \boldsymbol{\Omega}^H \right)$ is an $LK \times LK$ matrix. By taking the derivative of χ^{MMSE} in (A.9) with respect to $\mathbf{Q}^H$ and setting the result to zero, the sub-optimal MMSE compensation matrix, $\mathbf{Q}^{[\text{MMSE}]}$, is determined as shown in (3).

REFERENCES

[1] Y. Tian, X. Lei, Y. Xiao, and S. Li, "SAGE based joint timing-frequency offsets and channel estimation in distributed MIMO systems," *Elsevier Journal Computer Commun.*, vol. 33, no. 17, pp. 2125–2131, Jul. 2010.

[2] A. A. Nasir, H. Mehrpouyan, S. D. Blostein, S. Durrani, and R. A. Kennedy, "Timing and carrier synchronization with channel estimation in multi-relay cooperative networks," *IEEE Trans. Signal Process.*, vol. 60, no. 2, pp. 793–811, Feb. 2012.

[3] S. Ma, Y. Yang, and H. Sharif, "Distributed MIMO technologies in cooperative wireless networks," *IEEE Commun. Mag.*, vol. 49, no. 5, pp. 78–82, May 2011.

[4] M.-K. Chang and S.-Y. Lee, "Performance analysis of cooperative communication system with hierarchical modulation over Rayleigh fading channel," *IEEE Trans. Wireless Commun.*, vol. 8, no. 6, pp. 2848–2852, Jun. 2009.

[5] Y. Jing and B. Hassibi, "Distributed space-time coding in wireless relay networks," *IEEE Trans. Wireless Commun.*, vol. 5, no. 12, pp. 3524–3536, Dec. 2006.

[6] Y. Jing and H. Jafarkhani, "Using orthogonal and quasi-orthogonal designs in wireless relay networks," *IEEE Trans. Inf. Theory*, vol. 53, no. 11, pp. 4106–4118, Nov. 2007.

[7] X. Li, Y. C. Wu, and E. Serpedin, "Timing synchronization in decode-and-forward cooperative communication systems." *IEEE Trans. Signal Process.*, vol. 57, no. 4, pp. 1444–1455, Apr. 2009.

[8] F. Tian, X.-G. Xia, and P. C. Ching, "Signal detection in a cooperative communication system with multiple CFOs by exploiting the properties of space-frequency codes," in *Proc. IEEE ICC*, 2008.

[9] H. Wang, X.-G. Xia, and Q. Yin, "Computationally efficient equalization for asynchronous cooperative communications with multiple frequency offsets," *IEEE Trans. Wireless Commun.*, vol. 8, no. 2, pp. 648–655, Feb. 2009.

[10] D. Veronesi and D. L. Goeckel, "Multiple frequency offset compensation in cooperative wireless systems," in *Proc. IEEE GLOBECOM*, 2006.

[11] A. A. Nasir, S. Durrani, and R. A. Kennedy, "Achieving cooperative diversity with multiple frequency offset estimation," in *Proc. IEEE ICSPCS*, 2011.

[12] Z. Li and X.-G. Xia, "An alamouti coded OFDM transmission for cooperative systems robust to both timing errors and frequency offsets," *IEEE Trans. Wireless Commun.*, vol. 7, no. 5, pp. 1839–1844, May 2008.

[13] O.-S. Shin, A. M. Chan, H. T. Kung, and V. Tarokh, "Design of an OFDM cooperative space-time diversity system," *IEEE Trans. Veh. Technol.*, vol. 56, no. 4, pp. 2203–2215, Jul. 2007.

[14] Q. Huang, M. Ghogho, J. Wei, and P. Ciblat, "Practical timing and frequency synchronization for OFDM based cooperative systems," *IEEE Trans. Signal Process.*, vol. 58, no. 7, pp. 3706–3716, Jul. 2010.

[15] Y. M. Bishop, S. E. Fienberg, and P. W. Holland, *Discrete Multivariate Analysis: Theory and Practice.* Springer, 2007.

[16] O. Besson and P. Stoica, "On parameter estimation of MIMO flat-fading channels with frequency offsets," *IEEE Trans. Signal Process.*, vol. 51, no. 3, pp. 602–613, Mar. 2003.

[17] H. Meyr, M. Moeneclaey, and S. A. Fechtel, *Digital Communication Receivers, Synchronization, Channel Estimation, and Signal Processing*, J. G. Proakis, Ed. Wiley Series in Telecom. and Signal Processing, 1998.

[18] S. M. Kay, *Fundamentals of Statistical Signal Processing: Estimation Theory.* NJ: Prentice Hall, 1993.

[19] N. Moller, "On Schoonhage's algorithm and subquadratic integer gcd computation," *Mathematics of Computation*, vol. 77, pp. 589–607, Jan. 2008.